Stationary Frame Current Regulation of PWM Inverters With Zero Steady-State Error

Daniel Nahum Zmood, *Student Member, IEEE* and Donald Grahame Holmes, *Member, IEEE*

Abstract—Current regulators for ac inverters are commonly categorized as hysteresis, linear PI, or deadbeat predictive regulators, with a further sub-classification into stationary ABC frame and synchronous d–q frame implementations. Synchronous frame regulators are generally accepted to have a better performance than stationary frame regulators, as they operate on dc quantities and hence can eliminate steady-state errors. This paper establishes a theoretical connection between these two classes of regulators and proposes a new type of stationary frame regulator, the P+Resonant regulator, which achieves the same transient and steady-state performance as a synchronous frame PI regulator. The new regulator is applicable to both single-phase and three phase inverters.

Index Terms—ac current control, current control, resonant regulator, linear PI, single phase current regulation, stationary frame regulators, synchronous frame regulators, three phase current regulation.

I. INTRODUCTION

CURRENT regulation is an important issue for power electronic converters, and has particular application for high performance motor drives and boost type pulsewidth modulated (PWM) rectifiers. Over the last few decades considerable research has been done in this area for voltage source inverters, and from this work three major classes of regulator have evolved, i.e., hysteresis regulators, linear PI regulators, and predictive regulators [1]. These classes can be further divided for three phase regulators into stationary and synchronous d–q reference frame implementations by applying ac machine rotating field theory [2], [3].

In general, three phase *stationary frame* regulators are regarded as being unsatisfactory for ac current regulation since a conventional PI regulator in this reference frame suffers from significant steady-state amplitude and phase errors. In contrast, synchronous frame d–q regulators can achieve zero steady-state error by acting on dc signals in the rotating reference frame, and are therefore usually considered to be superior to stationary frame regulators. However, a synchronous frame regulator is more complex, as it requires a means of transforming a measured stationary frame ac current (or error) to rotating frame dc quantities, and transforming the resultant control action back to the stationary frame for execution. These transformations can
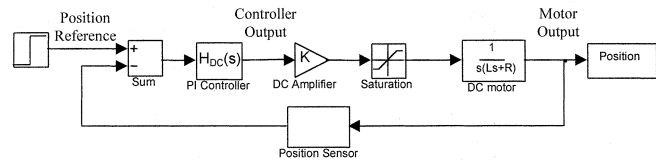
Fig. 1. DC motor servo control system.

introduce errors if the synchronous frame identification is not accurate.

In this paper, concepts taken from carrier-servo control systems [4], [5] are used to develop a new P+Resonant stationary frame regulator for single and three phase systems which achieves virtually the same steady-state and transient performance as a synchronous frame PI regulator. The paper explores the relationship between stationary and synchronous frame regulators from a control system and signal processing perspective, and shows how the regulator transfer function can be transformed instead of the ac current error, to achieve a stationary frame linear PI current regulator with zero steady-state error and a good transient performance. The steady-state performance of this new regulator is similar to that achieved in [6] but it is more stable and has a superior transient performance [7]. A further significant advantage of this regulator is its application to single-phase current regulated systems, where synchronous frame transformations are more difficult to apply.

II. SERVO CONTROL SYSTEMS V'S HYBRID CONTROL SYSTEMS

Servo control systems are sometimes called dc control systems because the controlled quantity (or its integral) is dc under steady-state conditions. The steady-state error for such systems is determined by their open loop gain at dc, while their transient responses are determined predominantly by the frequency responses at the system crossover frequency. Fig. 1 shows a block diagram for a typical dc motor position servo control system, where the forward path is composed of the dc regulator compensation network—$H_{DC}(s)$, a saturating dc amplifier with gain K and a dc motor. Position feedback is commonly provided by a dc potentiometer.

For an ac control system, such as a three phase current regulated VSI, the actuating and transducer signals are sinusoidal quantities. With a stationary frame (usually PI) regulator, the entire control loop then operates on ac quantities, and is subject to steady-state error. The conventional explanation for this steady-state error is that the stationary frame regulator can only provide finite gain at nonzero frequencies [8], [9]. In contrast, a synchronous frame d–q regulator operates on both ac and dc
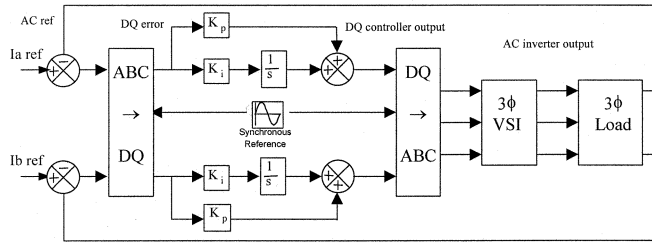
Fig. 2. Hybrid synchronous frame current control system.

signals, and can be categorized as a hybrid control system. In particular, as the synchronous frame control loop regulator operates on dc quantities, it can provide infinite gain and hence achieve zero steady-state error.

The major difference between these two systems is the inclusion of a demodulator, which shifts the sidebands of the ac reference sinusoid in the stationary frame to the dc frequency region in the synchronous frame. This then allows the regulator PI compensation network to be implemented as a dc network, with its output being subsequently remodulated to re-introduce the reference frequency into the final controller output signal. Fig. 2 shows the block structure of a three phase d–q synchronous frame PI current regulator to illustrate these features.

Fig. 3 shows the open loop time and spectral response at various points along the block diagram of a dc servo system, and illustrates the low-pass filtering effects of the regulator PI network and the dc steady-state nature of the system.

Fig. 4 shows the open loop time and spectral response of a hybrid control system at a number of points along the block diagram. From this figure, it can be seen how the envelope of the amplitude modulated ac reference input exists in the frequency domain as sidebands about the fundamental reference frequency. The demodulation and re-modulation effect of the synchronous frame transformation in converting these sidebands into a base-band frequency envelope in the synchronous frame can be clearly seen in Fig. 4, together with the low-pass filtering effect of the synchronous frame regulator dc compensation network.

III. REGULATOR COMPENSATION STRATEGIES

The key limitation of most stationary frame linear current regulation systems is their inability to eliminate steady-state error. The three phase synchronous d–q PI regulator solves this problem by shifting the base-band information back to dc where conventional dc regulator networks can be used. For such conventional linear controllers, it is the integral term that provides infinite gain at dc and therefore achieves zero steady-state error. The proportional term is frequency independent and so whether it is implemented inside or outside the frequency transformation is decided by convenience. For smaller integral gains the transient response of the regulation system will be almost totally determined by the proportional term while the steady-state response is determined by the integral term, and so the two can be analyzed separately. Their combined effect need only be taken into account when considering the system stability.

An alternative approach, derived from servo control theory and the insight gained from Figs. 3 and 4, is to frequency transform the dc type regulator network into an equivalent ac regulator, instead of demodulating the reference sideband signal spectra. If this is possible then the control response achieved by a synchronous frame d–q PI regulator would be achievable in the stationary frame without requiring the demodulation and modulation process. Essentially, the transformed regulator would directly operate on the ac error using sidebands about the reference fundamental. Two approaches for control of an *ac* sinusoidally excited current regulator can be considered based on these concepts.

A. Conventional Hybrid Compensation System

This type of regulator has been well documented in the literature for three phase systems as a synchronous frame current regulator, although it is usually not viewed from the perspective of frequency shifting the input reference spectrum to a dc base-band. The advantage of this approach is that it allows the use of well known dc compensation methods to develop the synchronous frame transfer function, and these are easier to design and construct than ac compensators. The disadvantages are the additional complexity and computation required to add a demodulator and modulator to the control system, and the need to develop an accurate synchronous frame reference signal. Two approaches are possible.

1) Product Demodulation: This method is directly related to the traditional Parks Transformation for three phase systems and its fundamentals are well known in spectrum analysis theory. The signal is multiplied by reference sine and cosine waveforms which shift any harmonic content at that frequency to dc and the double-frequency. This is illustrated mathematically as

$$x_c(t) = x(t) \cdot \cos(\omega_o t) = x(t) \cdot \frac{e^{j\omega_o t} + e^{-j\omega_o t}}{2} \quad (1)$$

$$x_s(t) = x(t) \cdot \sin(\omega_o t) = x(t) \cdot \frac{e^{j\omega_o t} - e^{-j\omega_o t}}{2}. \quad (2)$$

Taking the Fourier transformation, these become

$$X_c(\omega) = \tfrac{1}{2} \left[X(\omega + \omega_o) + X(\omega - \omega_o) \right]$$

$$X_s(\omega) = \frac{1}{2j} \left[-X(\omega + \omega_o) + X(\omega - \omega_o) \right].$$

Now if $x_c(t) = \cos(\omega_o t)$, the real and imaginary components have information present at dc and at the double-frequency. If these signals are low-pass filtered the output signals become

$$Y_c(\omega) = \tfrac{1}{2} X_c(0)$$

$$Y_s(\omega) = \frac{1}{2j} X_s(0) \quad (3)$$

which are the real and imaginary components of $x(t)$ in phasor or spectral form.

Fig. 5 illustrates how the basic demodulation concept defined by (1)–(3) can be implemented to achieve PI regulation for a single-phase sinusoidally excited system. The low-pass filter used to extract the real and imaginary terms is replaced with an
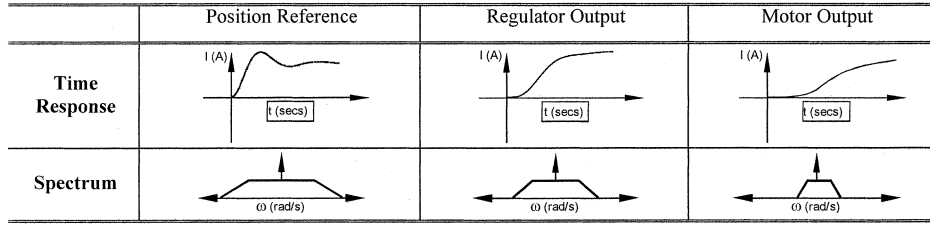
	Position Reference	Regulator Output	Motor Output
Time Response			
Spectrum			

Fig. 3.   Time Response and spectral range of signals within dc motor servo control system.

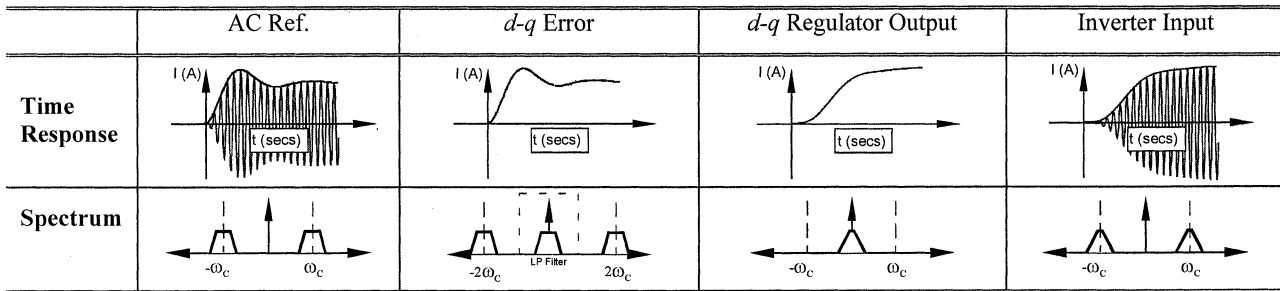|	AC Ref.	*d-q* Error	*d-q* Regulator Output	Inverter Input
Time Response				
Spectrum				

Fig. 4.   Time response and spectral range of signals within hybrid control system.

Fig. 5.   Demodulating single-phase integral block.

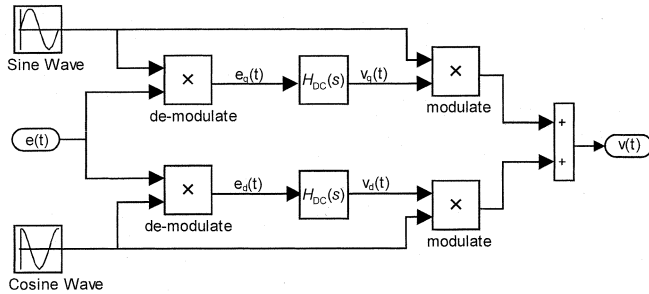Fig. 6.   Vestigial sideband demodulation integral block.

integrator, which plays the dual role of providing integral action and filtering the double-frequency components for the demodulated signal. (Using a low-pass filter as well, would seriously degrade the stability of the overall control system as the low-pass filter and integrator would add $180°$ of phase lag between them.) Fig. 5 can be considered a hybrid regulator replacement block for the integral term of a PI regulator, since as previously mentioned, the proportional term can be implemented outside the demodulating block without changing its influence.

2) Single or Vestigial Sideband Demodulation: This technique phase shifts the error signal by $90°$ to allow the use of a conventional stationary to rotating frame transformation and is illustrated in Fig. 6 [10]. However, the introduction of the All-Pass network to produce the required phase shift introduces additional dynamics compared to the previous strategy, which leads to a deterioration in stability and transient performance. Hence it will not be discussed further in this paper.

B. AC Compensation System

An stationary frame ac regulator that does achieve zero steady-state error and can be directly applied to ac signals is not well known in power electronic systems, but has been developed in car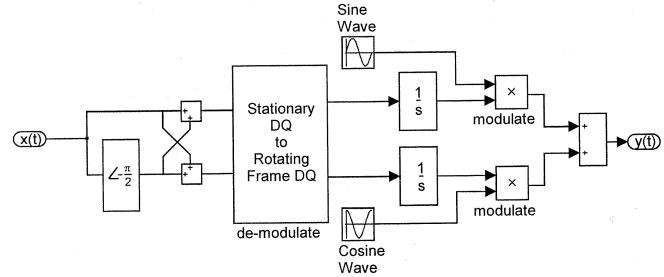rier-servo control theory. The principle is to transform a desired dc compensation network into an equivalent ac compensation network, so that it has the same frequency response characteristic in the bandwidth of concern. The required exact transformation (developed in the Appendix) is

$$H_{\mathrm{AC}}(s) = \frac{H_{\mathrm{DC}}(s + j\omega_o) + H_{\mathrm{DC}}(s - j\omega_o)}{2}. \qquad (4)$$

If $H_{\mathrm{DC}}(s)$ is a low-pass transfer block, this transformation results in a low-pass to band-pass or frequency shifting transformation to the frequency ω_o.

A alternative to (4), when the reference signal bandwidth is small in comparison to the reference frequency itself, is to use the low-pass to band-pass technique developed in network synthesis, i.e.,

$$H_{\mathrm{AC}}(s) = H_{\mathrm{DC}}\left(\frac{s^2 + \omega_o^2}{2s}\right). \qquad (5)$$

In some applications (5) provides a more convenient implementation.

A stationary frame controller implemented using the transfer function $H_{\mathrm{AC}}(s)$ will have an **equivalent** frequency response to a synchronous frame controller implemented using the transfer
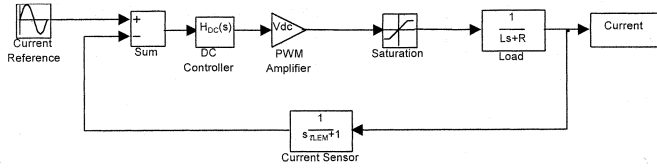
Fig. 7. Model of a current regulated PWM inverter.

function $H_{DC}(s)$, since these functions have been shown to be mathematically identical in the Appendix. Therefore the transient response of the two controller implementations will be identical regardless of whether they are implemented in the stationary frame as an ac compensator or in the synchronous frame as a dc compensator.

IV. REALIZATION OF THE NEW AC COMPENSATION SYSTEM

A major objective for ac current regulators is to achieve zero phase and magnitude error. Using ac compensation, this objective can be achieved by transforming a dc compensator that achieves this goal into an equivalent ac compensator. Fig. 7 shows a typical dc compensated current regulation system, where for convenience the asymmetrically modulated PWM converter stage has been modeled as a simple saturating gain stage.

For the dc system, a conventional PI transfer function achieves the desired objective of zero steady-state error. Hence using the transformation of (5), an equivalent ac compensator would have an open loop transfer function of

$$H_{DC}(s) = K_p + \frac{K_i}{s} \qquad (6)$$

$$H_{AC}(s) = K_p + \frac{2K_i s}{s^2 + \omega_o^2} \qquad (7)$$

which has a frequency and phase response shown in Fig. 8. Note that the proportional gain term K_p has been kept separate from the transformation process as discussed earlier.

The closed loop transfer function for the linear model of Fig. 7 with this compensator is given by

$$T(s) = \frac{H_{AC}(s)V_{DC}(s\tau_{LEM}+1)}{R+sL+H_{AC}(s)V_{DC}(s\tau_{LEM}+1)}. \qquad (8)$$

From (8), the closed loop transfer function of the system will clearly approach unity at the fundamental reference (target) frequency with no phase or magnitude error in the output waveform since the magnitude of $H_{AC}(s)$ becomes infinite at this frequency. However, the realization of an ideal dc integrator or its corresponding ac equivalent loss-less resonant transfer function is sometimes not possible due to component tolerances in analog systems and finite precision in digital systems. But an ideal integrator is often approximated by a low-pass transfer function such as

$$H_{DC}(s) = K_p + \frac{K_i \cdot \omega_c}{s + \omega_c}. \qquad (9)$$

This transforms using (5) into

$$H_{AC}(s) = K_p + \frac{2K_i \omega_c s}{s^2 + 2\omega_c s + \omega_o^2} \qquad (10)$$
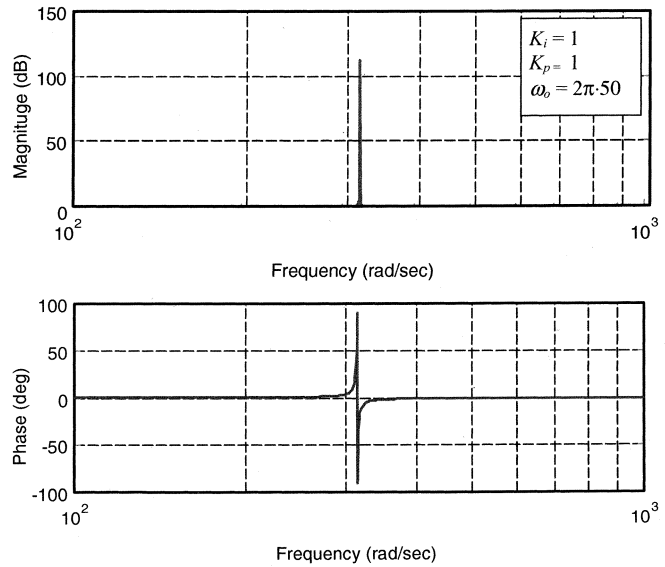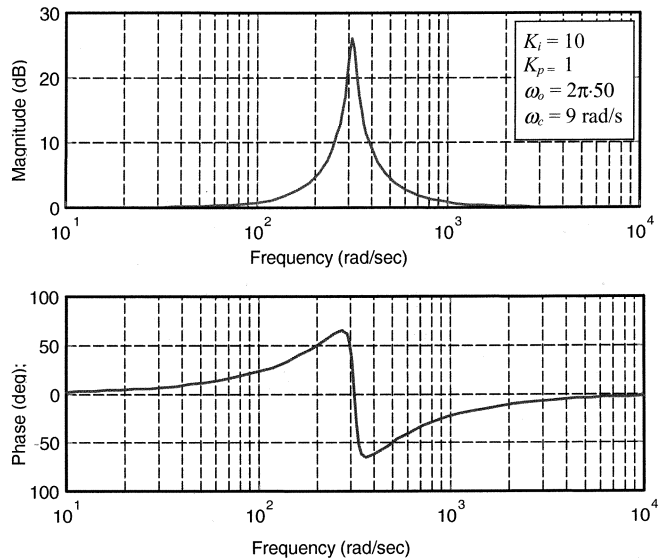

Fig. 8. Bode plot of ac compensator from (7).

Fig. 9. Bode plot of ac compensator from (10).

where ω_c is the lower breakpoint frequency of the dc transfer function. This network has a frequency and phase response as shown in Fig. 9. The steady-state output phase and magnitude error achieved by this compensator will still be approximately zero, provided $H_{AC}(s)$ continues to achieve a relatively high gain at the reference frequency.

Constructing the current regulator in the stationary reference frame has the advantage of requiring much less signal processing than the synchronous frame demodulation approaches, and it is also less sensitive to noise. Furthermore, the application of this implementation to single-phase systems is straightforward and undifferentiated from its application to three phase systems. But it does require for variable frequency applications that the resonant frequency of the ac compensator is adjusted to match the required output fundamental frequency. However, this is not as challenging as it may first appear, since a number
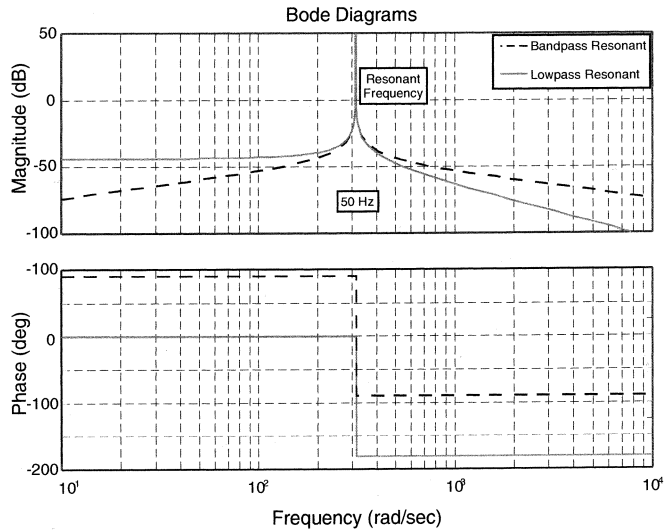
Fig. 10.   Frequency responses of loss-less resonant terms for (7) and (11).

Fig. 11.   Open loop Bode plots of proportional and resonant regulators.

of standard techniques already exist in signal processing theory to operate across variable frequencies.

For digital implementations, it is simply required to re-calculate the digital filter co-efficient to suit the target frequency. This co-efficient could be calculated either as part of the control loop calculation, or as a background task without requiring significant CPU resources (this was the approach used in the experimental digital implementation), depending on the speed of response required. In either case, the level of computation required is (at worst) similar to that required for a stationary to synchronous frame transformation process.

Band pass operation at a variable frequency is a straightforward requirement for analog signal processing systems, and hence is not considered further in this paper. One approach for example would be to use a switched capacitor filter, where the center frequency is simply adjusted by varying the switching frequency of the filter.

It is noted also that the new controller presented in this paper has a transfer function similar to that presented by Sato *et al.* [6], which has a resonant transfer function given by

$$H_{\mathrm{AC}}(s) = K_p + \frac{K_i \omega_o}{s^2 + \omega_o^2}. \qquad (11)$$

Sato's transfer function also has infinite gain at the resonant frequency and hence achieves zero steady-state error when used as a current regulator. But it is not based on an exact transformation from the equivalent synchronous frame controller, and in particular introduces a phase shift of $180°$ into the system, compared to the $90°$ shift of the P+Resonant system, as illustrated in Fig. 10. In closed loop operation this $180°$ phase shift results in a poorer phase margin and a poor transient performance for this regulator compared to the approach presented here [7].

V. STABILITY CONSIDERATIONS

A major benefit of being able to express the frequency response of the new regulator in the transfer function form of (7) or (10), is that linear control theory can be used to investigate the stability of current regulation systems based on this approach.
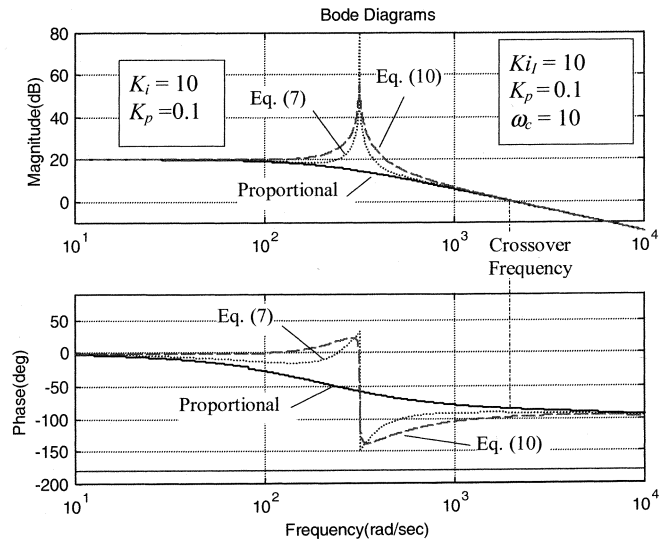
Using conventional Bode plots, it is straightforward to show that the regulator integral gain can be made sufficiently large to essentially remove all steady-state error (similar to the effect of the finite integral gain that most practical dc compensators can achieve), without any significant stability limitations.

Note:

The current sensor was modeled by a single pole low-pass filter with breakpoint at 100 kHz. This component has little effect on the magnitude response of the system but the additional phase shift it introduces can have a significant effect on the system stability.

It should be noted that the resonant terms provide very little gain outside their band-pass region due to their narrowband frequency response. Hence, to achieve a reasonable transient response a proportional gain term is also required. Fig. 11 shows the magnitude and phase bode diagrams for a simple proportional regulator and the two regulators described by (7) and (10).

For $K_p = 0.1$ the magnitude crossover frequency (i.e., where the regulator gain becomes less than 1) of the simple proportional regulator occurs at 3 kHz, as indicated in Fig. 11. The phase plot shows a phase margin of more than $100°$ at this frequency so the system is clearly stable. The introduction of the resonant regulator terms radically alters the Bode plots at the resonant frequency but has little effect at the crossover frequency for the regulator parameters chosen. Hence, both resonant regulators remain stable below the crossover frequency because the phase shift is always less than $180°$. Fig. 11 also shows that most of the high frequency or transient response of the regulator is determined by the proportional gain since the resonant regulator magnitude responses return to that of a simple proportional system at higher frequencies. So, the larger the proportional gain the faster will be the transient response.

This suggests a simple two-step design procedure for the complete regulator. Firstly, chose a proportional gain such that the regulator is stable and gives a good transient response. Then design a resonant component that gives the desired steady-state
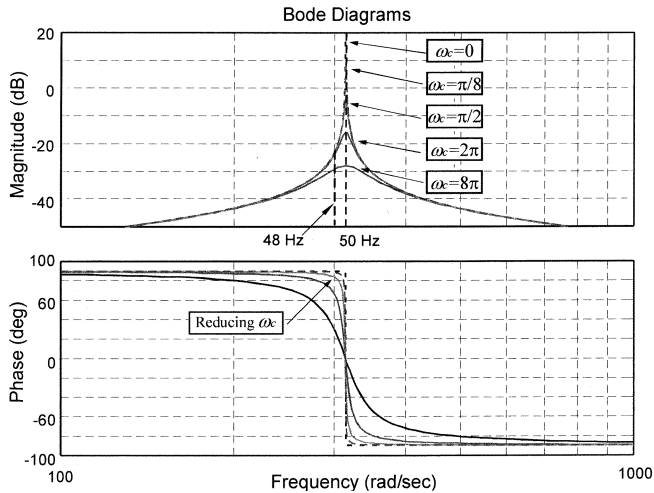
Fig. 12. Bode response of the resonant term for variation in ω_c and $K = 1$.

phase and amplitude error without making the phase margin too small.

A. Effect of the 3-dB Cut-Off Frequency

The low-pass 3-dB cut-off frequency ω_c appears to allow a degree of freedom in the design of the resonant frequency responses. It is often used as a measure of the bandwidth of a filter and therefore increasing its size would appear to broaden the effect of the high gain created by the resonant term. This in turn would appear to increase the regulator robustness by reducing the sensitivity of the system to variations in the fundamental frequency.

Unfortunately, in reality this advantage does not exist, as can be shown by setting the gain K_i to K/ω_c so that the gain variation in (10) is removed and the effect of changes in ω_c can be more easily observed. For the damped resonant term generated by the LP–BP transformation, the gain at the resonant frequency is given by

$$H_{AC}(j\omega_o) = \frac{2Kj\omega_o}{-\omega_o^2 + 2j\omega_o\omega_c + \omega_o^2} = \frac{1}{\omega_c} \quad (12)$$

which is clearly inversely dependent on the value of ω_c. Hence it can be seen that varying ω_c simply changes the peak amplitude of the resonant term at the resonant frequency, without affecting the shoulder frequency gain. The Bode response of (12) for a range of values of ω_c is illustrated in Fig. 12.

At frequencies greater than or less than the resonant frequency all the plots converge to the 20 dB per decade asymptotic response regardless of the value of ω_c. The major difference between the different plots is the increasing peak amplitude at the resonant frequency for smaller values of ω_c. This illustrates that the infinite gain benefit of the ideal resonant term only occurs at the resonant frequency and any perturbation will lead to a reduction of the generated gain. Hence, the P+Resonant regulator is potentially sensitive to the alignment between the regulator's resonant frequency and the fundamental frequency of the inverter system. The only way of reducing this sensitivity is to increase the regulator gain K, which uniformly increases the gain response but does not effect the shape of the frequency

response. For example, if the reference frequency were 48 Hz rather than 50 Hz the loss-less resonant term attenuates the signal by more than 20 dB, as can be seen in Fig. 12. Increasing ω_c (to supposedly increase the filter bandwidth) actually makes things worse as this flattens the frequency response, further reducing the gain of the resonant term.

One major conclusion from this consideration is that there is no benefit to be gained in using the damped resonant implementations. If an ideal resonant term is realizable it is preferable, and if a damped term must be used it should be implemented with as small a value of ω_c as possible.

B. PWM Constraint

A fundamental constraint of PWM systems is that the maximum rate of change of the reference should not equal or exceed that of the carrier signal or for digital systems the maximum frequency of the reference should be less than half the sample frequency. For an analog system this requirement must be met for a fixed PWM switching frequency. For the simple proportional feedback system and an analog sine-triangle PWM system, the critical gain is

$$K_p(\max) = \frac{4Lf_{carrier}}{V_{dc}} \quad (13)$$

where L is the system inductance, $f_{carrier}$ is the carrier frequency of the PWM system and V_{dc} is the dc bus voltage.

If the load is purely resistive a low-pass filter can be placed after the current sensor or as part of the compensator to restrict the rate of change of the error signal. A similar constraint exists for a regular sampled PWM system.

VI. SIMULATION RESULTS

The current regulators discussed in this paper have been investigated and compared in simulation, using a MATLAB-based discrete and continuous time step representation of the physical switched inverter system. This simulation gives a very realistic output without the usual simplifying assumptions that are present in many linear simulations, and in particular allows delays within a real digital regulator system to be incorporated without difficulty.

Fig. 13 shows the simulated steady-state and transient response that can be achieved with the new P+Resonant regulator for both a low and a high backemf load, and Table I defines the regulator parameters for these results (and also the previous stability simulations). In both cases it can be seen that there is no steady-state error during continuous modulation, and only a slight error just after the transient event occurs. This error is caused by the settling time of the resonant part of the regulator transfer function.

Fig. 14 shows the simulated steady-state and transient response of the stationary frame, synchronous frame and resonant regulators driving a four-pole permanent magnet motor. The elimination of steady-state error for the resonant regulator can be clearly seen, and its transient response is almost identical to that of a synchronous frame regulator.

One limitation with P+Resonant scheme that has been identified from simulation is that an exponentially decaying transient
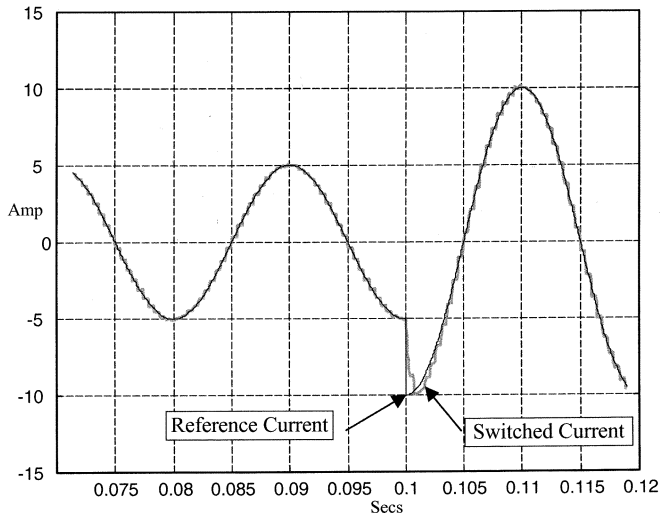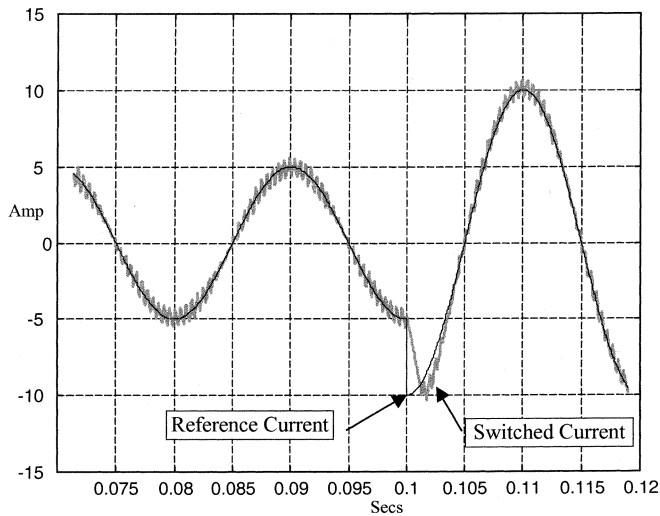
Fig. 13. (a) Simulated response of ac compensator, zero backemf. (b) Simulated response of ac compensator, 0.7-pu backemf.

TABLE I
SIMULATION AND EXPERIMENTAL SINGLE PHASE PARAMETERS

LOAD	Inductance	5 mH
	Resistance	2 Ohms
Supply Volts		200 Vdc
Regulator Gains	Proportional	0.1
	Resonant	10
Switching Freq		1 kHz

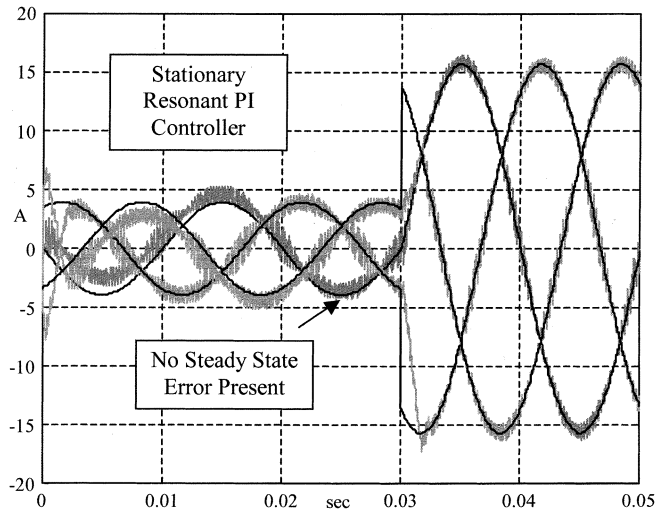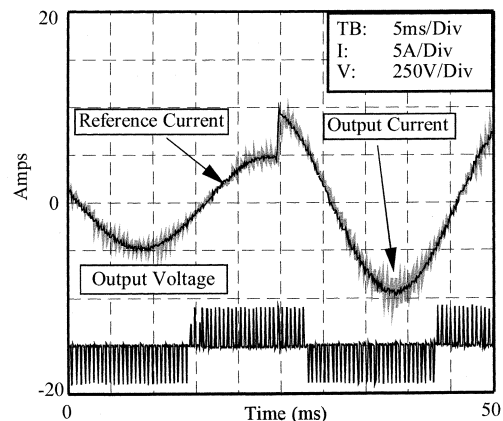Fig. 14. Simulation response of three phase ac compensator driving ac motor.

Fig. 15. Experimental response of ac compensator, zero backemf.

can occur during step changes due to the existence of a transient negative sequence component. This effect can be observed in the start up process of Fig. 14, where the simulation has saturated just after startup because of initialization errors in the system variables. The result is a small transient phase and magnitude error for the next cycle or so and can be minimized by anti-integral-wind-up logic. The exact cause of this error, and its relationship to transient errors in a synchronous frame current regulator, will be addressed in a future paper.

VII. EXPERIMENTAL RESULTS

The new P+Resonant regulator has been experimentally verified by in an analog single-phase form and digital three phase form. The analog regulator was prototyped on a breadboard with the resonant term realized using a UAF41 a universal filter IC and driving a simple R-L load with the parameters described in Table I. Fig. 15 shows the results are very similar to the equivalent simulated results with the regulator achieving zero steady-state error and a rapid transient response.

The digital regulator was implemented in the abc frame using a TMS320F240 DSP based VSI regulator firstly driving an R-L load, and then an induction motor load, with parameters as listed in Table II. Fig. 16 shows the experimental response for the conventional stationary frame PI regulator with an R-L load and clearly illustrates the steady-state error associated with this regulator. Fig. 17 shows the transient and steady-state response for the new P+Resonant regulator driving an induction motor (backemf load) with the elimination of steady-state error clearly illustrated. It also indicates that the new P+Resonant regulator can be tuned to exhibit minimal overshoot and an excellent rise time, very similar to that predicted by simulation.

TABLE II
THREE PHASE EXPERIMENTAL AND SIMULATION SYSTEM PARAMETERS

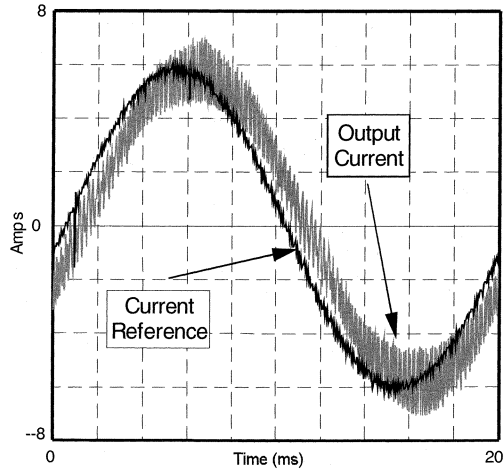| PER PHASE LOAD	L	7 mH
	R	0.5 Ω
Supply Volts		580 Vdc
Fund. Freq.		50Hz
Switching Freq		5 kHz

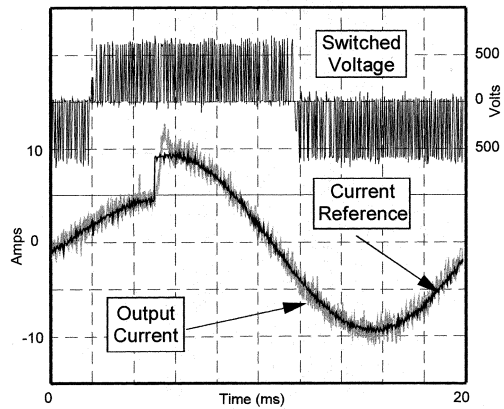Fig. 16. Experimental steady-state response for conventional stationary PI current with an R-L load.

Fig. 17. Experimental steady-state and transient responses for new P+Resonant current regulator driving an Induction Motor.

VIII. SUMMARY

Synchronous frame current regulators are usually accepted as being superior to stationary frame regulators because the synchronous transformation of the ac current error allows conventional dc compensation strategies to be used to achieve zero steady-state error. In this paper, this advantage is shown to derive from the carrier demodulation process inherent in the synchronous transformation. Based on this understanding, single-phase regulators with zero steady-state error are developed both in the dc (synchronous frame equivalent) region and in the stationary frame. It is then shown how a equivalent stationary frame current regulator with theoretically identical performance can be implemented by transforming the regulator compensation network rather than the current error signal. The result is a stationary frame current regulator that achieves zero

steady-state error, and is equally applicable to single-phase or three phase systems. The new regulator has been fully evaluated both in simulation and experimentally using both analog and digital techniques.

APPENDIX
DEVELOPMENT OF AC TRANSFORMATION

The single-phase synchronous frame regulator of Fig. 5 can be described in the time-domain by

$$v_{AC}(t) = \{[e_{AC}(t) \cdot \cos(\omega_o t)] * h_{DC}(t)\} \cdot \cos(\omega_o t) + \{[e_{AC}(t) \cdot \sin(\omega_o t)] * h_{DC}(t)\} \sin(\omega_o t) \quad (A1)$$

where $*$ denotes a convolution product. From this description, the aim is to determine a transfer function $H_{AC}(s)$ which provides the same frequency responses as (A1), but without the modulation and de-modulation processes. The system in this form can be represented by

$$V_{AC}(s) = H_{AC}(s) E_{AC}(s). \quad (A2)$$

The time domain description of (A2) is

$$v_{AC}(t) = e_{AC}(t) * h_{AC}(t) \quad (A3)$$

where ω_o is the fundamental frequency. To simplify the following mathematics two functions are defined:

$$h_{DC}(t) * (e_{AC}(t) \cdot \cos(\omega_o t)) \equiv f_1(t)$$
$$h_{DC}(t) * (e_{AC}(t) \cdot \sin(\omega_o t)) \equiv f_2(t). \quad (A4)$$

The Laplace transforms of these functions are

$$\begin{aligned} F_1(s) &= \ell\{h_{DC}(t) * (e_{AC}(t) \cdot \cos(\omega_o t))\} \\ &= H_{DC}(s) \cdot \ell\{e_{AC}(t) \cdot \cos(\omega_o t)\} \\ &= \tfrac{1}{2} H_{DC}(s)\{E_{AC}(s + j\omega_o) + E(s - j\omega_o)\} \quad (A5) \end{aligned}$$

$$\begin{aligned} F_2(s) &= \ell\{h_{DC}(t) * (e_{AC}(t) \cdot \sin(\omega_o t))\} \\ &= H_{DC}(s) \cdot \ell\{e_{AC}(t) \cdot \sin(\omega_o t)\} \\ &= \frac{j}{2} H_{DC}(s)\{E_{AC}(s + j\omega_o) - E(s - j\omega_o)\}. \quad (A6) \end{aligned}$$

The mathematical description of the regulator (A1) is now broken into two components, A and B and the Laplace transform of each component is derived using the functions f_1 and f_2 and the modulation theorem of the Laplace transform, i.e.,

$$\begin{aligned} A &= \ell\{[(e_{AC}(t) \cdot \cos t(\omega_o t)) * h_{DC}(t)]\cos(\omega_o t)\} \\ &= \ell\{f_1(t) \cdot \cos(\omega_o t)\} \\ &= \tfrac{1}{2}\{F_1(s + j\omega_o) + F_1(s - j\omega_o)\} \\ &= \tfrac{1}{4}\left\{ \begin{array}{l} H_{DC}(s + j\omega_o)\{E_{AC}(s + 2j\omega_o) + E_{AC}(s)\} \\ + H_{DC}(s - j\omega_o)\{E_{AC}(s) + E_{AC}(s - 2j\omega_o)\} \end{array} \right\} \end{aligned}$$
$$(A7)$$

$$\begin{aligned} B &= \ell\{[(e_{AC}(t) \cdot \sin t(\omega_o t)) * h_{DC}(t)]\sin(\omega_o t)\} \\ &= \ell\{f_1(t) \cdot \sin(\omega_o t)\} \\ &= \frac{j}{2}\{F_1(s + j\omega_o) - F_1(s - j\omega_o)\} \\ &= \tfrac{1}{4}\left\{ \begin{array}{l} -H_{DC}(s + j\omega_o)\{E_{AC}(s + 2j\omega_o) - E_{AC}(s)\} \\ + H_{DC}(s - j\omega_o)\{E_{AC}(s) - E_{AC}(s - 2j\omega_o)\} \end{array} \right\}. \end{aligned}$$
$$(A8)$$

Both A and B contain the dc and double-frequency error component terms $E_{AC}(s)$ and $E_{AC}(s + 2j\omega_o)$ considered in the Type I regulator discussion, as well as frequency shifted versions of the dc regulator function $H_{DC}(s + 2j\omega_o)$.

Finally the transformed version of the dc transfer function $H_{DC}(s)$ is produced by summing A and B

$$
\begin{aligned}
V_{AC}(s) &= A + B \\
&= \tfrac{1}{4}\left\{2\left[H_{DC}(s + j\omega_o) + H_{DC}(s + j\omega_o)\right]\right\} \cdot E_{AC}(s) \\
&= \tfrac{1}{2}\left[H_{DC}(s + j\omega_o) + H_{DC}(s - j\omega_o)\right] \cdot E_{AC}(s)
\end{aligned}
$$
$$(A9)$$

hence

$$
H_{AC}(s) = \tfrac{1}{2}\left[H_{DC}(s + j\omega) + H_{DC}(s - j\omega)\right]. \quad (A10)
$$

Equation (A10) allows the generation of the frequency response of the regulator (A1) for any given dc regulator transfer function $H_{DC}(s)$. The analysis also illustrates the cancellation of the double-frequency components in (A9) generated by the demodulation process as long as $H_{DC}(s)$ is the same for both signal paths and there are no distortions in the multiplications.

REFERENCES

[1] M. P. Kazmierkowski and L. Malesani, "Current control techniques for three-phase voltage-source PWM converters: A survey," *IEEE Trans. Ind. Electron.*, vol. 45, pp. 691–703, Oct. 1998.

[2] C. D. Schauder and R. Caddy, "Current control of voltage source inverters for fast four quadrant drive performance," *IEEE Trans. Ind. Applicat.*, vol. IA-18, pp. 163–171, May/Apr. 1982.

[3] T. M. Rowan and R. J. Kerkman, "A new synchronous current regulator and an analysis of current regulated PWM inverters," *IEEE Trans. Ind. Applicat.*, vol. IA-22, pp. 678–690, July/Aug. 1986.

[4] J. J. D'Azzo and C. H. Houpis, *Feedback Control System Analysis and Synthesis*, 2nd ed. Tokyo, Japan: McGraw-Hill, 1966.

[5] G. J. Murphy, *Control Engineering*. Princeton, NJ: Van Nostrand, 1959.

[6] Y. Sato, T. Ishizuka, K. Nezu, and T. Kataoka, "A new control strategy for voltage-type PWM rectifiers to realize zero steady-state control error in input current," *IEEE Trans. Ind. Applicat.*, vol. 34, pp. 480–486, May/June 1998.

[7] S. Fukuda and T. Yoda, "A novel current-tracking method for active filters based on a sinusoidal internal model for PWM invertors," *IEEE Trans. Ind. Applicat.*, vol. 37, pp. 888–895, May/June 2001.

[8] H. Nagase, Y. Matsuda, K. Ohnishi, H. Ninomiya, and T. Koike, "High-performance induction motor drive system using a PWM inverter," *IEEE Trans. Ind. Applicat.*, vol. IA-20, pp. 1482–1489, Nov./Dec. 1984.

[9] D. M. Brod and D. W. Novotny, "Current control of VSI-PWM inverters," *IEEE Trans. Ind. Applicat.*, vol. IA-21, pp. 562–570, May/June 1985.

[10] Y. Xiaoming, J. Allmeling, W. Merk, and H. Stemmler, "Stationary frame generalized integrators for current control of active power filters with zero steady-state error for current harmonics of concern under unbalanced and distorted operation conditions," in *Proc. Conf. IEEE/IAS Annu. Meeting*, 2000, pp. 2143–2150.

Daniel Nahum Zmood (S'97) received the B.S. degree (with honors) in electrical engineering from Monash University, Melbourne, Australia, in 1996 and the Ph.D. degree in power electronics from the Department of Electrical and Computer System Engineering, Monash University, Clayton, Australia, in 2003.

In 1996, he worked for 12 months as a Researcher in the Power Electronics Group, Monash University, on switch mode power supply design and power cable field measurement and prediction. His major fields of interest include the modulation and control of PWM current source inverters, current regulation of sinusoidal converters, switch mode power supply design and control and signal processing. He has also engaged in consulting and contract work in the area of power electronics. He has published 12 papers at international conferences and in professional journals.

Mr. Zmood is currently a member of the IEEE Industry Applications, IEEE Power Electronics, and IEEE Industrial Electronics Societies.

Donald Grahame Holmes (M'87) received the B.S. degree and M.S. degree in power systems engineering from the University of Melbourne, Melbourne, Australia, in 1974 and 1979, respectively, and the Ph.D. degree in PWM theory for power electronic converters from Monash University, Clayton, Australia, in 1998.

He worked for six years with the local power company developing SCADA systems for power transmission networks, before returning to the University of Melbourne as a faculty member. In 1984, he moved to Monash University to work in the area of power electronics, and he is now an Associate Professor at this university in this area. He heads the Power Electronics Research Group, Monash University, where he manages graduate students and research engineers working together on a mixture of theoretical and practical R&D projects. The present interests of the group include fundamental modulation theory, current regulators for drive systems and PWM rectifiers, active filter systems for quality of supply improvement, resonant converters, current source inverters for drive systems, and multilevel converters. He has a strong commitment and interest in the control and operation of electrical power converters. He has made a significant contribution to the understanding of PWM theory through his publications and has developed close ties with the international research community in the area. He has published over 100 papers at international conferences and in professional journals, and regularly reviews papers for all major IEEE TRANSACTIONS in his area.

Dr. Holmes is a member of the IPC and IDC Committees, IEEE Industrial Applications Society, and is Webmaster for the IEEE Power Electronics Society.